3138–3146 Nucleic Acids Research, 1994, Vol. 22, No. 15

Mcp and *Fab-7*: molecular analysis of putative boundaries of *cis*-regulatory domains in the bithorax complex of *Drosophila melanogaster*

François Karch, Mireille Galloni, László Sipos[1], János Gausz[1], Henrik Gyurkovics[1] and Paul Schedl[2,*]

Department of Zoology and Animal Biology, University of Geneva, 154 rte de Malagnou, 1224 Geneva, Switzerland, [1]Institute of Genetics, Biological Research Center, Hungarian Academy of Sciences, PO Box 521, 6701 Szeged, Hungary and [2]Department of Biology, Princeton University, Princeton, NJ 08544, USA

Received April 8, 1994; Revised and Accepted June 21, 1994 EMBL accession nos X77898, X78983

ABSTRACT

A very large *cis*-regulatory region of ~300 kb is responsible for the complex patterns of expression of the three homeotic genes of the bithorax complex *Ubx*, *abd-A* and *Abd-B*. This region can be subdivided in nine parasegment-specific regulatory subunits. Recent genetic and molecular analysis has revealed the existence of two novel *cis*-regulatory elements *Mcp* and *Fab-7*. *Mcp* is located between *iab-4* and *iab-5*, the parasegment-specific regulatory subunits which direct *Abd-B* in parasegments 9 and 10. Similarly, *Fab-7* is located between *iab-6* and *iab-7*, the parasegment 11 and 12-specific regulatory units. *Mcp* and *Fab-7* appear to function as domain boundaries that separate adjacent *cis*-regulatory units. We report the analysis of two new *Mcp* mutant deletions (*Mcp*^{H27} and *Mcp*^{B116}) that allow us to localize sequences essential for boundary function to a ~0.4 kb DNA segment. These essential sequences closely coincide to a ~0.3 kb nuclease hypersensitive region in chromatin. We also show that sequences contributing to the *Fab-7* boundary appear to be spread over a larger stretch of DNA, but like *Mcp* have an unusual chromatin structure.

INTRODUCTION

During the early development of *Drosophila melanogaster*, the embryo is subdivided into 14 units called parasegments (PS: for review, see 1, 2). Each parasegment acquires its specific identity through the action of the homeotic genes in the *Antennapedia* and bithorax complex (BX-C). The BX-C contains three genes, *Ubx*, *abd-A* and *Abd-B* which are responsible for the identities of PS5 to PS14. These parasegments will form the posterior half of the thorax and all of the abdominal segments of the adult fly (for review, see 3–6). *Ubx*, *abd-A* and *Abd-B* encode homeodomain proteins and they are expressed in intricate temporal and spatial patterns in an overlapping set of parasegments (7–19). A ~300 kb *cis*-regulatory region is responsible for generating the complex patterns of bithorax gene expression. Genetic analysis has suggested that this very large *cis*-regulatory region is sub-divided into nine parasegment-specific units—*abx/bx*, *bxd/pbx*, *iab-2*, *iab-3*, *iab-4*, *iab-5*, *iab-6*, *iab-7* and *iab-8*. As shown in Fig. 1A, these parasegment-specific *cis*-regulatory units are arranged in the same order along the chromosome as the parasegments they affect (Fig. 1A; 20–25). On the proximal side of the complex, *abx/bx* and *bxd/pbx* control the expression of the *Ubx* homeotic gene in PS5 and PS6, respectively (18, 26). In the middle of the complex, *iab-2*, *3* and *4* specify the appropriate patterns of expression of *abd-A* in PS7, 8 and 9, respectively (12, 27, 28). *Abd-B*, which has several alternate promoters, is controlled by the *cis*-regulatory units on the distal side of the complex (Fig. 1A). A short *Abd-B* transcript (class A) is required to produce the morphological diversity of the region from PS10 through 13 (10, 11, 13, 19, 29–31). The *iab-5*, *6* and *7* parasegment-specific units regulate expression of this *Abd-B* transcript in PS10,11 and 12, respectively (21, 28, 29), while in PS13 its expression is probably controlled by a PS13-specific regulatory element (*iab-8;* unpublished data). In PS14, a collection of *Abd-B* transcripts (class B, C and gamma) initiating from at least three other promoters are expressed (10, 11, 13, 19, 29, 31); however, the PS14-specific regulatory elements controlling these promoters have not been identified.

Loss-of-function mutations in one of these nine parasegment specific *cis*-regulatory units transforms the corresponding parasegment into a copy of the parasegment immediately anterior. Consistent with this transformation in segmental identity, the normal temporal and spatial pattern of the relevant BX-C homeotic gene is replaced by an expression pattern which mimics that found in the parasegment immediately anterior. For example, the *iab-5 cis*-regulatory region is responsible for the expression of the short *Abd-B* transcription unit in a few cells of the epidermis

*To whom correspondence should be addressed

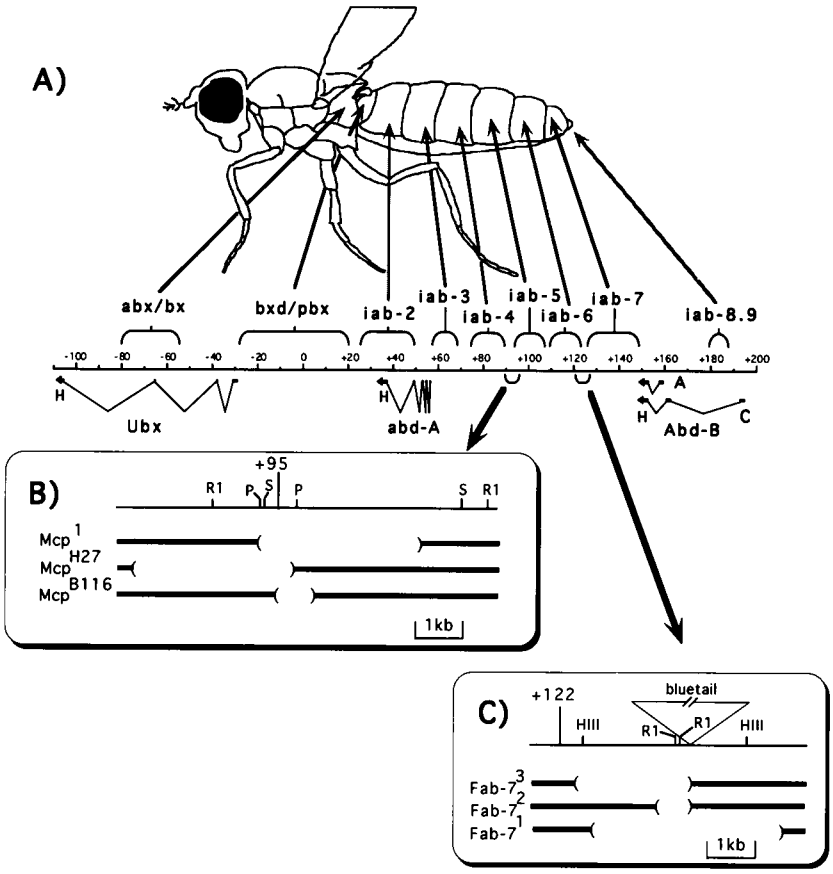

Figure 1. Synopsis of the BX-C and molecular maps of the Mcp and Fab-7 boundaries. (**A**) The thin horizontal line represents the 300 kb of genomic DNA. The *Ubx*, *abd-A* and *Abd-B* transcription units are drawn below the genomic DNA line, the H indicating the positions of the homeoboxes. Horizontal brackets above the genomic DNA lines represent the approximate extent of the parasegment-specific *cis*-regulatory units. The arrows point towards the parasegments of a fly in which the *cis*-regulatory units function. (**B**) Molecular map of the *Mcp* region. The thin horizontal line represents a magnification of the genomic DNA shown in part A around position +95. Some of the restriction sites in this region are indicated. The extent of the deficiencies in Mcp^{1}, Mcp^{H27} and Mcp^{B116} are shown by brackets. (**C**) Molecular map of the *Fab-7* region. The thin horizontal line represents a magnification of the genomic DNA shown in part A around position +122. Some of the restriction sites in the region are shown. The extent of the deficiencies in $Fab\text{-}7^{1}$, $Fab\text{-}7^{2}$ and $Fab\text{-}7^{3}$ are indicated by brackets. Also indicated is the insertion site for the *bluetail* transposon.

and central nervous system (CNS) in PS10. This *Abd-B* expression disappears in *iab-5* mutant embryos resulting in the transformation of PS10 into PS9 or, in the adult fly, of the 5th abdominal segment (A5) into A4 (21, 28). Similarly, a mutation that removes much of the *iab-7 cis*-regulatory region ($iab\text{-}7^{\Delta Sz}$) results in the transformation of PS12 into PS11 (or in the adult A7 into A6). In this case, instead of the normal *Abd-B* expression pattern in PS12, a PS11-like pattern, which is generated by *iab-6*, is observed (21, 22, 28).

Current models for the functioning of these *cis*-regulatory regions divided the regulation of the bithorax complex into two phases, initiation and maintenance. During the initiation phase, gap and pair-rule gene products are thought to interact with target sequences in each *cis*-regulatory unit. These interactions activate the *cis*-regulatory units in appropriate parasegments, where they direct the initial expression of one of the three homeotic genes (32–42). As the gap and pair-rule gene products begin to disappear mid-way through embryogenesis, there is transition from the initiation to the maintenance phase. During this transition, the activity state of the *cis*-regulatory units which was established in each parasegment during initiation is 'fixed' through the combined action of the *trithorax* and *Polycomb* group gene products. These proteins then function to maintain this activity state during the remainder of development (25, 26, 40, 43–53).

In addition to the 9 *cis*-regulatory units which direct the parasegmental expression of the three homeotic genes, genetic studies have identified two unusual *cis*-acting elements, *Mcp* and *Fab-7*. *Mcp* is located between the *iab-4* and *iab-5 cis*-regulatory units, while *Fab-7* is located between *iab-6* and *iab-7*. Unlike loss-of-function mutations in the *cis*-regulatory units, which show a transformation of the affected parasegment into the parasegment immediately anterior, deletions that remove either of these elements have an opposite, gain-of-function phenotype; they transform the affected parasegment into a copy of the parasegment immediately posterior. In the Mcp^{1} deletion, PS9 is replaced by a duplication copy of PS10. In the adult fly, Mcp^{1} results in the development of A4 into a copy of A5 (24). The gain-of-function phenotype of Mcp^{1} appears to be due to the inappropriate activation of the *iab-5 cis*-regulatory unit in PS9 where *iab-4* normally functions. Consistent with this suggestion, *Abd-B*, which is not normally transcribed in PS9, is expressed in PS9 in a PS10-like pattern in Mcp^{1} mutant embryos (21, 28). Deletions

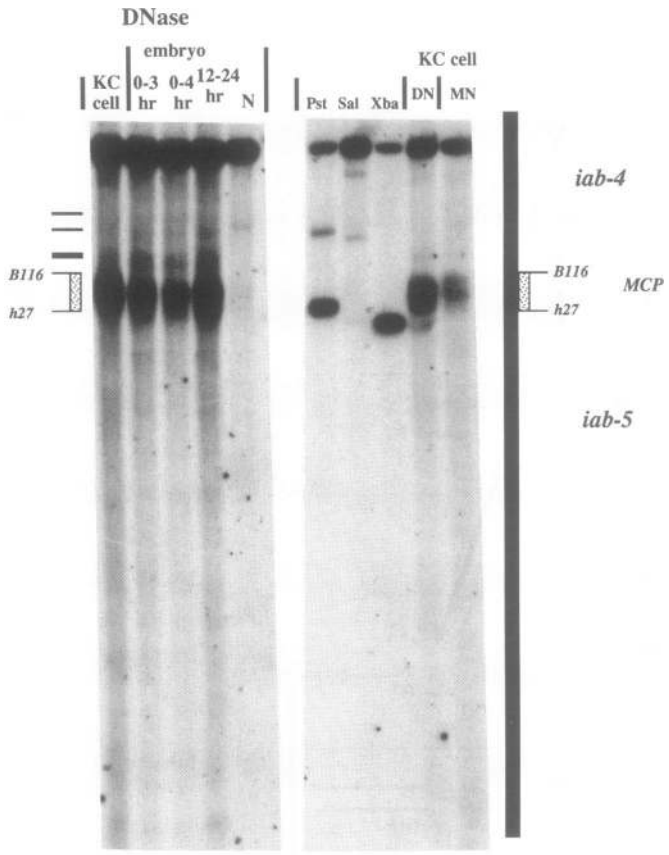

Figure 2. DNase hypersensitive sites in the *Mcp* boundary. In the experiments shown in this Figure, DNA samples from DNase I (DN) or micrococcal nuclease (MN) digests of nuclei from embryos (0−3, 0−4 and 12−24 hr collections) and KC cells were restricted with Eco R1 and electrophoresized on 40 cm agarose gels. After blotting to nitrocellulose filters, the DNA probed with an Eco R1−Sph I fragment from the distal side of the Eco R1 fragment. N is a naked DNA control in which total genomic DNA was digested partially the DNase I. Micrococcal nuclease naked DNA controls were not included in the experiments shown here; however, in contrast to the chromatin digests, there are multiple sites for micrococcal nuclease across the 6.0 kb Eco R1 fragment in naked DNA. To align as closely as possible the *Mcp* chromatin structure with the *Mcp* sequence, total genomic DNA was digested to completion with Eco R1 and partially with Pst I, Sal I, or Xba I. (Lanes containing a 2.0 kb MW ladder were also included in these and other gels, but are not shown in the photos presented here.) In other experiments the nuclease cutting pattern was aligned using partial digestion with other restriction enzymes. The weakly labeled Sal I fragment just below the full length Eco R1 fragment arises from Eco R1 cleavage at a second Sal I site which is located on the distal edge of the 6 kb fragment, very close to the distal Eco R1 site. The probe used for indirect end-labeling extends beyond this Sal I site. Proximal and distal limits of the *B116* and *H27* deletions are indicated by the stipled area. Bars indicate positions of minor nuclease hypersensitive sites. The proximal most site at ~625 bp is not indicated.

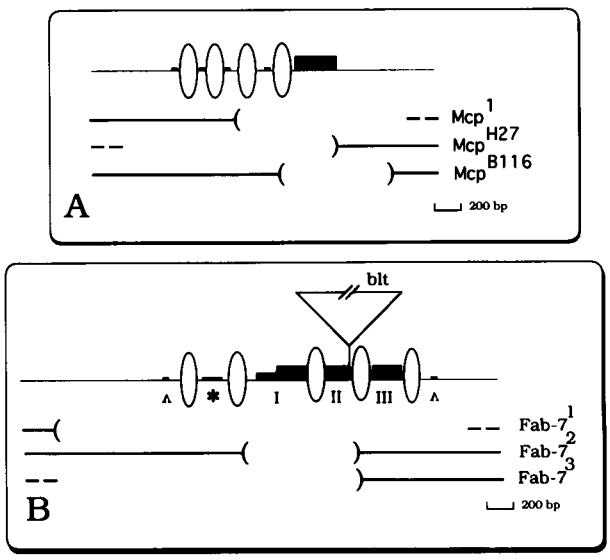

Figure 3. Chromatin structure of the *Mcp* and *Fab-7* boundaries. (**A**) Chromatin structure of the *Mcp* boundary. The thin top line represents the sequenced region presented in Fig. 4A. The black rectangles indicate the extent of the hypersensitive regions. Strong hypersensitive sites are shown by thick black rectangles, while weak hypersensitive regions are indicated by thin black rectangles. The ovals indicate nuclease resistant DNA segments that could be packaged into nucleosome core particles. The different *Mcp* boundary deletions are shown below the DNA line. (**B**) Chromatin structure of the *Fab-7* boundary. The chromatin structure of the *Fab-7* region was analyzed previously in 22, and the results are summarized here. The thin top line represents the sequenced region presented in Fig. 4B. The ovals indicate nuclease resistant regions that could contain nucleosome core particles. The different *Fab-7* boundary deletions are shown below the DNA line.

that remove *Fab-7* transform PS11 into PS12 in the embryo, and in the fly A6 into a copy of A7 (23). In this case, the transformation appears to be due to the inappropriate activation of the *iab-7 cis*-regulatory unit in PS11 where *Abd-B* is normally controlled by *iab-6*. Indeed, in *Fab-7* mutant embryos the pattern of *Abd-B* protein expression in PS11 is identical to that found in PS12 (22).

Since the dominant gain-of-function phenotype of the *Fab-7* deletion mutants can be reverted by second site mutations that eliminate *either iab-6* or *iab-7* function, the inappropriate activation of *iab-7* in PS11 would appear to involve interactions between the *iab-6* and *iab-7 cis*-regulatory units (23). A similar interaction between *iab-4* and *iab-5* appears to be required for the dominant gain-of-function phenotype associated with the Mcp^1 deletion (24). These findings have led to the suggestion that *Mcp* and *Fab-7* may correspond to the boundaries of *cis*-regulatory domains (22, 23, 54). In this model, the boundary elements are responsible for ensuring that the different *cis*-regulatory units in the bithorax complex are functionally autonomous. Consequently, when one of these insulating elements is deleted, adventitious interactions between adjacent *cis*-regulatory units are possible.

In previous studies (22) we examined the chromatin structure of the *Fab-7* DNA segment and characterized three *Fab-7* deletion mutants by genomic Southerns. These studies indicated that the sequences essential for *Fab-7* function spanned a DNA segment of about 3 kb and have an unusual chromatin structure in embryos and tissue culture cells. In this paper, we have characterized the original *Mcp* allele, Mcp^1, as well as two new *Mcp* mutants. This analysis maps the sequences required for *Mcp* function to a DNA segment of ~0.4 kb. Moreover, we find that the essential sequences closely coincide with a ~0.3 kb nuclease hypersensitive region. We also report here the sequence of *Fab-7* and of the various *Fab-7* mutants, and compare the sequence and chromatin organization of the *Fab-7* element with *Mcp*.

EXPERIMENTAL PROCEDURES

Drosophila cultures

Fly stocks were maintained on standard yeast-cornmeal medium. Mcp^1 is described in 24, $Fab\text{-}7^1$ in 23, $Fab\text{-}7^2$ and $Fab\text{-}7^3$ are

described by 22. Mcp^{H27} and Mcp^{B116} were found among the progeny of two genetic screens for mutations affecting BX-C function. Mcp^{H27} was induced by X-rays (4,000 rads; 1000 rads/min, 0.5mm Al filter) on an *Fab-7* bearing chromosome and was recovered in a screen of ~38,000 flies for *Fab-7* revertants. Mcp^{B116} was induced on an Oregon R chromosome with X-rays (using similar conditions) in a screen for second site suppressors of *Fab-7*. Approximately 20,000 flies were examined in this screen. Both mutations were identified on the basis of their dominant *Mcp* phenotype.

Whole genome Southern, construction of genomic libraries and phage analysis

Whole genome Southern, construction of genomic libraries and phage analysis were performed as described in 20, 23 and 24. Partially Sau3A digested genomic DNA fragments (from $McpH^{27}$, $McpB^{116}$, $Fab7^{2}$ and $Fab\text{-}7^{3}$ homozygous flies) were fractionated on sucrose gradients. Fragments between 15–20 kb in length were inserted into the BamH1 sites of EMBL3 (55). Mcp^{1} and $Fab\text{-}7^{1}$ were already cloned as described 23 and 24.

DNA sequencing

Appropriate DNA fragments from the genomic clones were subcloned into pEMPL8, pEMBL9, Bluescript KS$^-$ or SK$^-$ vectors. Sequencing reactions were performed on single strand DNA preparations using universal or specific primers and the Sequenase kit (USB) . Subclones were also generated by unidirectional digestion with Exo 3 exonuclease using a protocol from Promega (56).

Chromatin studies

Nuclei were prepared from 0–3 hr, 0–4 hr, 0–12 hr and 12–24 hr mass collected embryos and from *Drosophila* tissue culture cells as described in 57. The nuclei were incubated for different lengths of time with DNase I or micrococcal nuclease, and the digested DNA was then purified by proteinase K treatment and phenol extraction as described in 57. Total genomic DNA was also isolated from nuclei (not treated with nuclease). For indirect end-labeling experiments, the DNA samples were restricted with the appropriate restriction enzyme, electrophoresized on 40 cm agarose gels, and blotted to nitrocellulose filters.

RESULTS

Chromatin structure of the *Mcp* boundary

Putative boundaries of chromatin domains in number of systems have been found to be associated with unusual chromatin structures. In chicken, a boundary from the 5′ end of the globin gene complex contains a 'constitutive' nuclease hypersensitive site that is present in chromatin from many different tissues (58). Similarly two putative boundaries from the 87A7 heat shock locus of *Drosophila*, scs and scs', are defined by a pair of rather broad nuclease hypersensitive sites which flank a short nuclease resistant core (59–61). This is also true for the *Fab-7* boundary in the bithorax complex, which is thought to separate the *iab-6* and *iab-7* *cis*-regulatory domains; the DNA segment required for *Fab-7* function contains three prominent nuclease hypersensitive sites (22). These observations suggested that it would be of interest

A

```
                                                                                                    100
GAATTCCGCT CGGAAAGGGA AGAAGTTCTG TGGCTTACTG AGTAAAGCGG ATTAAACTTT GATTGTCCCC AAAAGTTATG TGATGGCAAT TATAATCATA
                                                                                                    200
AAACTTTGAA ATAAATGTGT AACTTATTCA TTTGCACACG GTTTTCAATT TTTGATTATT CTGGAAAATT GCTATTTAGG ATGATTTGTA TGTGTACTTT
                                                                                                    300
AAAACAGAAA TAGATTAAAT AAAGTTCTGC TATACATGAC ATTTTAGAAA AATAAATATT GACTATCTTT GGTATACAAT TTCAGAAATA AGACAATTCC
                                                                                                    400
ATTTTAAAAT GTTAAATATT TGATTAATTA TATATACAGC TAAACTTGAA ATGCACGAGT TCCTGGAATG AGTAGATATT AATTTAAATT AATCCCATGC
                                                                                                    500
TACCGCTCAG TTAATTTAAA TTATATAAGT TGGTACTTAA ATTATGTAAA TTGTCTTGTC AAAGAATTTT TATGAACGAT AACAATTAAT AATAATTAGT
                                                                                                    600
ATTTAAAAAG GTGTATTTGG CGATTTTGTG TATATTAAAA AACATGACGC ACCTTACGCA AATGAATGAA CATTGTCATT AGCCGAAAAA AGTGTCGCCA
                                                                                                    700
TATTTGTGTT TAAAATACAA ATTATAATAA TCAAATAACC ATTACTCAGA GCTTGCCTGA AACGAGGCGA GGAAAAAATG ATTTCGAAAT CGCTTATGAA
                                                                                                    800
ATATAATTGG CTAATTTAGC AAGCCTCAAT ATAAAGTATA AGCATTCAAT TTACGATCTG AGTCAGCCGG AATCGAAACA GCATTATTCG CCGGAGATAA
                                                                                                    900
CGAATGGCGA GTGCAGAACG TCCTTTAGCG GAGTGCTCCG CCAACAGGTT CGCGATAAGG CGGGGCCATT AAGAGGCACC TGTCAGTGCG ACCCTCCCCG
                                                                                                   1000
CCCACCATTG TCGTCATAAA GCGTCAAGTT TATGCCGAAA ATTGAAATTA ATATGCCGTT CGATGGCTCG ATTAAAATGC GCTAAACGAA ACCGGCAAGT
                                                                                                   1100
ACGGGGCAAG TATGACTCTA TATATGTATG TACACATGTA TGTGTATCGG GATCAGGGCG TGGCACCTGA AATGCTGTAA AAGCCAGCTG CAGACTTAAA
                                                                                                   1200
TTGATTTAAA GTTTGCTGCC TCTTCAACGA CAGTTCAAAT GCAAATTGGC TGGTCGACCT GCCCGTTTTC CGTTTTATTG CGAATATTAA ATGAAATTAA
                                                                                                   1300
TGAAATTTTC TGCGCCATAA TCCTTTGCAA AACGCATAAA TTTGCTCATT AAGTGTGCGC AAATATTGTA TGTATCCGCT CCGCTAAAAG GTCTATATAC
                                                                                                   1400
TTTATATACT TGTATTGATT TTTAAGCTCA GATAAATAAG CTCAGAGTAC ATAAGCGACG CCCAAAAAGC CCAAATGTAG AGCTTTTTCG AAATTAAACA
                                                                                                   1500
GAAAGTCGGG TCTGCAAATA AGGGCTTTTC TGGGGAAGAA ATAAATTATA TCTTAATAAA TATATTTTAA ACTTAACTCA GACTTGGATT TATTTTGAAC
                                                                                                   1600
TACACACTTA AGTGATTTAA ATAATTTTAA ATATATTTCT TACATAAATT TAGCCAATAT CCAAACCTTT TTGCGCTGGC GCCCCCTATT GTTTTTCTTT
                                                                                                   1700
CGCAGCTCAT GCTTTGCTGG CAACCCACCA GAGGACGCTC GCTGATTGAA TCGCATTACG CACACTTACA ACGATTGGGT TTTTCATGTG TTAGTGCGTG
                                                                                                   1800
AGAGTAAGTG AGACAACAGG CTTATTGATG TGGTCTTCCT CCTTACACAA AATACATGGC CGCGCGACAA AGATGGCAAC ATTGATGGCT GCCTCTGAAA
                                                                                                   1900
ACATGGCCTC TTTTTCCGAC ATTGTATCTG TGTGACGTTT GACTGCAGAT GCGTTTGTGT GGGTAGTATA TGTATCTTCT AGATTTAAGT CGATTTTGTC
                                                                                                   2000
AACTAATTTT GCGCTTTGTT ACCCCTGAAA ATGGGAGCTC ATGCGCAGTA TGCAGCTGGT GCGGAATTTT TCTAGATTTT TTTTCGGTTT TTTCTGCTCT
                                                                                                   2100
GCTTATCAGT TTATTGGACT GTAGTTAAAA CTTGCATGCA ATATTTAATG CGGGAAAATG AGAATGCAAA TTTTTGTGAA ATCTCTTTGG CTCTGACATG
                                                                                                   2200
TACCAAAATC CAAGTGCCTG ACTAAATTAA GTTTTTTTCT TTCTTCTTAC CCCAAAATCA AAACTTGATC CCAGCTATAT CGTGACACGT TCGCATTATG
                                                                                                   2300
CTGTCGAAAA TTGTCACATA AATCAATCAT ATTTATACAA ATGTCCCTGA TAGCCAAACC GCCCGCCACC AGTTGTTGAC AATATGCTAA TTTGCTTCGT
                                                                                                   2400
CTTTGTCTTG CCTTTTTGTC TGTCCATGCC CACGATAAGC AGTTGCTGAA AACGTGTTTT GGCATTTGAT TAGTTGCGAT ATGAGCGGCG GCAGAAGTTC
                                                                                                   2500
CAGGGAGCCA CGCAGCGAGT TCAAAATATT TCCAAACATG GAAGGTAATT CTGCCGGCTA ACGACTGGCA GCCATGTCAT TGGTCGCAGG TTGGTAAGCG

TAAGTATGTT TTCATGCCGA TGGATGTGGA ATTTTATAAC ATGGGCATAC GGACTGAGGC ATTTGCAGGT GTCAAATGG CGT
```

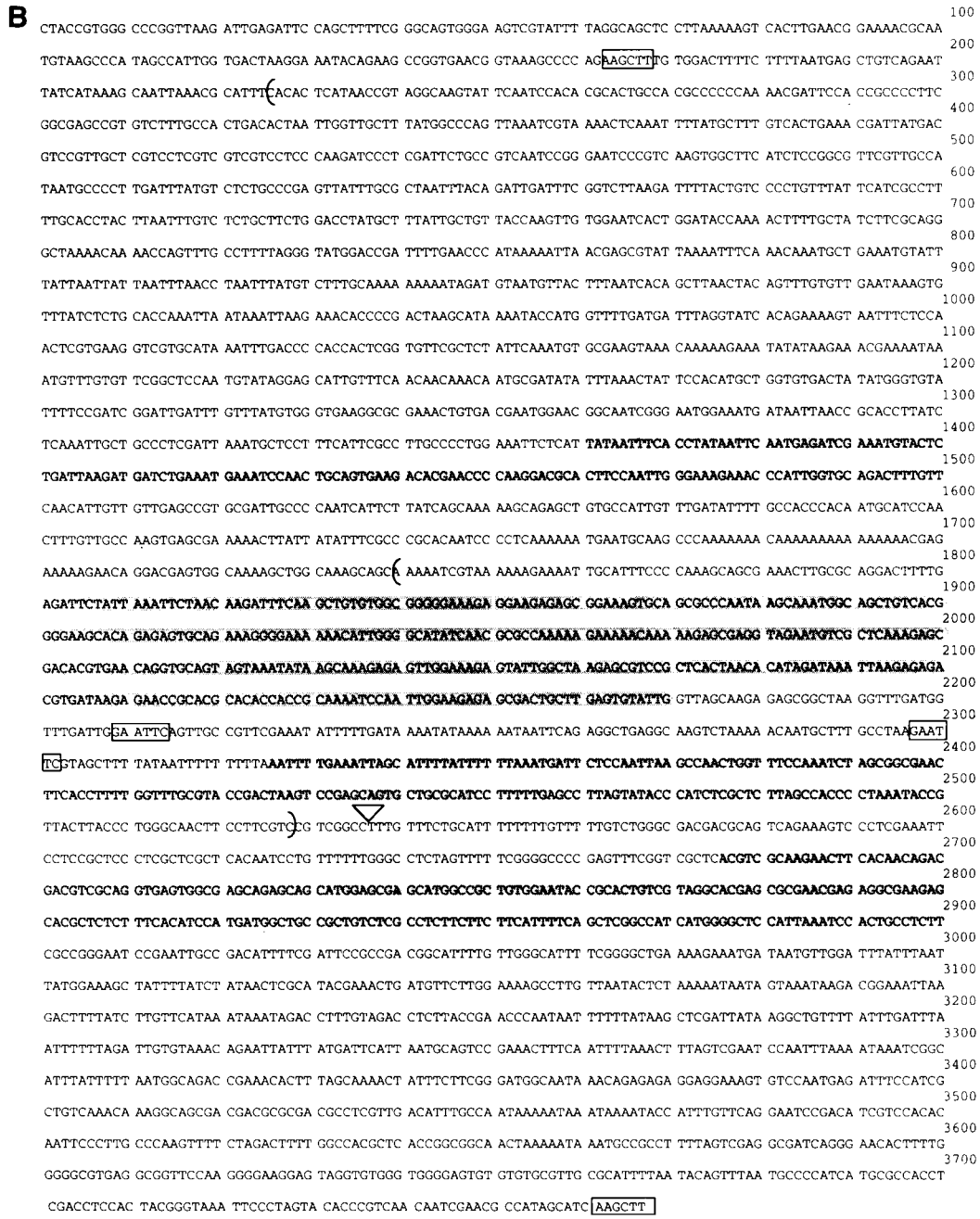

Figure 4. Nucleotide sequence of the *Mcp* and *Fab-7* boundaries. (**A**) The nucleotide sequence from the from the *Mcp* boundary is shown in the proximal to distal orientation, with *iab-4* to the left and *iab-5* to the right. Few landmark restriction sites to correlate with Fig. 1B and Fig. 2 are boxed (GAATTC=EcoR1; CTGCAG=Pst1; GTCGAC=Sal1; TCTAGA=Xba1; GCATGC=Sph1). Brackets indicate the proximal deletion breakpoint of Mcp^{1} at position 1027, the distal deletion breakpoint of Mcp^{H27} at position 1837 and the two deletion breakpoints of Mcp^{B116} at 1421 and 2289. The approximate positions of the nuclease hypersensitive regions are shown by gray boxes. EMBL #X778982. (**B**) The nucleotide sequence from the *Fab-7* boundary is shown in the proximal to distal orientation, with *iab-6* to the left and *iab-7* to the right. The HindIII (AAGCTT) and EcoR1 (GAATTC) sites shown in Fig. 1C are boxed. The insertion site of the *bluetail* transposon is indicated by a triangle at position 2536. The proximal deletion breakpoint of $Fab\text{-}7^{1}$ is indicated at position 225. The $Fab\text{-}7^{2}$ deletion from position 1739 to 2528 is due to an imprecise excision of the *bluetail* transposon. At the distal site, an insertion of 27 nucleotide of unknown origin occurred (CATCAGCAGGCATTTATTTCATCATG). The nuclease hypersensitive regions mapped in (22) are shown by gray boxes. EMBL #X78983.

to determine whether the *Mcp* boundary also has some type of unusual chromatin structure.

To examine the chromatin structure of the *Mcp* DNA segment, we prepared nuclei from 0–3 hr, 0–4 hr, and 12–24 hr embryos or from KC tissue culture cells and digested with either DNase I or micrococcal nuclease. The nuclease cleavage products in chromatin were analyzed by the indirect end-labeling technique. As indicated in the diagram in Fig. 1A, the original *Mcp* mutation, Mcp^{1}, is associated with a deletion of a ~3.6 kb DNA segment from the region in between the *iab-4* and *iab-5* *cis*-regulatory domains (from map position ~ +94 to +97.6 kb in the bithorax complex). This deletion is contained within a ~6.0

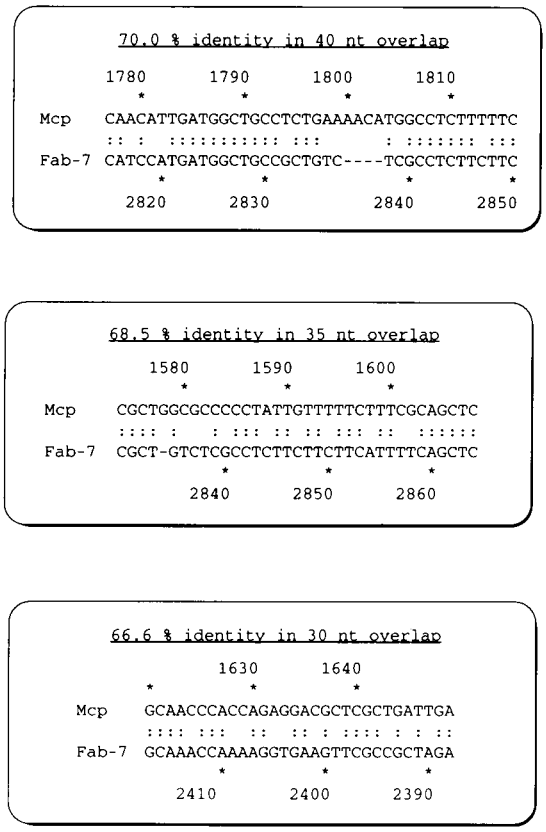

Figure 5. Regions of nucleotide sequence homology between the *Mcp* and *Fab-7* boundaries. These homologies have been found with *lalign* from the Pearson's programs. The value for the number of local alignments was 10 with the standard DNA scoring matrix.

kb Eco R1 fragment. For indirect end-labeling we used restriction fragment probes located to either the distal or proximal side of the Mcp^1 deletion. In the experiment shown in Fig. 2, Eco R1 restricted chromatin digests were probed with an Eco R1−Sph I fragment abutting the distal end of the 6.0 kb Eco R1 *Mcp* fragment. This displays the chromatin digestion products reading into the Mcp^1 deletion towards the centromere. In order to align the chromatin digestion products with the restriction map (and sequence) of the ~6.0 kb Eco R1 fragment, total genomic DNA was restricted to completion with Eco R1 and then subject to partial restriction digestion with restriction enzymes as indicated.

As illustrated in the autoradiograms in Fig. 2, the ~6. 0 kb Eco R1 fragment spanning the Mcp^1 deletion contains one very prominent nuclease hypersensitive region, as well as several minor nuclease hypersensitive sites. Essentially the same results were obtained using probes located to the proximal side of the 6.0 kb Eco R1 *Mcp* fragment (data not shown). In DNase I digests of chromatin, the major nuclease hypersensitive region (stipled area) covers a DNA sequence of more than 300 bp (see *Mcp* map in Fig. 3). The minor sites (indicated by bars) are considerably smaller and are spaced nucleosome length intervals (~200 bp) (see Fig. 3). Most of these DNase I cleavage products appear to be chromatin specific as they are not evident in control digests of naked DNA. The major hypersensitive region is cleaved extensively by DNase I in early (0−3, 0−4 hr) and late embryos (12−24 hr) and also in tissue culture cells (Fig. 2). It is also hypersensitive to micrococcal nuclease (see Fig. 2 and data not shown). Aligning the chromatin specific DNase I cleavage products with the restriction map of the ~6.0 kb Eco R1 fragment indicates that the major nuclease hypersensitive region plus the immediately adjacent minor hypersensitive site (thick bar) are removed by the Mcp^1 deletion (see Figs 1 and 3). Hence, like other putative domain boundaries, *Mcp* appears to be associated with an unusual chromatin structure.

Isolation and characterization of new *Mcp* mutations

To more precisely define the sequences required for *Mcp* function we isolated new *Mcp* alleles. Putative *Mcp* mutations can be readily identified on the basis of the cuticular pigmentation of adult male abdomens. In wild type males, there is a marked difference between the pigmentation of the 4th and 5th abdominal segments (A4 and A5 correspond to PS9 and PS10 respectively); A4 is unpigmented except for the very posterior border, while A5 is black. In Mcp^1, A4 is transformed into a copy of A5, and is darkly pigmented.

Two putative X-ray induced *Mcp* alleles, Mcp^{H27} and Mcp^{B116}, which exhibited this phenotypic transformation were identified in genetic screens (see Methods). Like the original Mcp^1 allele, they are dominant gain-of-function mutations, and genetic analysis indicated that both are very closely linked to the bithorax complex. Southern analysis of genomic DNA isolated from the two mutants revealed that both have lesions in the *Mcp* region of the bithorax complex. In Mcp^{H27} a DNA segment of approximately 2.8 kb extending roughly from position +92.5 kb to +95.5 kb is deleted. As indicated in the map in Fig. 1b, the Mcp^{H27} deletion overlaps the proximal end of the Mcp^1 deletion. Mcp^{B116} is also a deletion; however, it is smaller than either Mcp^1 or Mcp^{H27} removing a DNA segment of only about 1 kb located between ~ +95 kb and +96 kb. The Mcp^{B116} deletion is entirely included within Mcp^1, while it overlaps with the distal edge of Mcp^{H27}. Taken together, the genomic Southern analysis of the three deficiencies (see Fig. 1B) would map sequences essential for *Mcp* boundary function to a small region of less than 1 kb that is deleted in all three mutants. Moreover, in spite of the fact that both the extent and the end points of the deletions in these three mutants are different, their phenotypes are indistinguishable.

Sequence analysis of the *Mcp* DNA segment from wild type and *Mcp* mutants

To further characterize the *Mcp* boundary we sequenced a ~2.5 kb DNA segment from the *Mcp* region. The wild type *Mcp* sequence together with relevant restriction sites is presented in Fig. 4A. Also indicated in this figure are the approximate positions of the major chromatin specific nuclease hypersensitive region, and of the minor hypersensitive sites. These nuclease hypersensitive sites were aligned with the DNA sequence using the partial restriction enzyme digests in Fig. 2 as reference markers. This analysis indicates that the major hypersensitive region spans a DNA segment extending from approximately 1,540 bp to 1,860 bp (see also Fig. 3A). The first minor hypersensitive site on the proximal side is at ~1,325 bp, the second at ~1,050 bp, while the third and fourth at ~825 bp and ~625 bp.

To more closely correlate the sequences (and chromatin structures) required for *Mcp* boundary function we cloned DNA

segments from the three *Mcp* mutants and determined the proximal breakpoint of Mcp^{1} (24), the distal breakpoint of Mcp^{H27}, and both breakpoints of the smallest deficiency, Mcp^{B116}. These breakpoints are indicated in the wild type sequence (Fig. 4A). If one takes into account only the breakpoints of the smallest deficiency Mcp^{B116}, then sequence essential for *Mcp* function would be located between 1422 bp on the proximal side and 2289 on the distal side. This DNA segment includes the major nuclease hypersensitive region together with some 429 bp of DNA just distal to the hypersensitive region (see diagram in Fig. 3A). By contrast, sequences just proximal to the major nuclease hypersensitive region, including all of the minor nuclease hypersensitive sites, are not in themselves sufficient to confer boundary function. It is possible to further refine the DNA segment essential for boundary function by determining the minimal region of overlap between the three *Mcp* deficiencies. The proximal endpoint of the overlap is defined by the proximal Mcp^{B116} breakpoint at 1,421 bp, while the distal endpoint is defined by the distal breakpoint of Mcp^{H27} at 1,837 bp. As indicated in Figs 3A and 4A, these endpoints closely match the limits of the major chromatin hypersensitive region, and would raise the possibility that this unusual chromatin structure corresponds to the *Mcp* boundary.

Nucleotide sequence and chromatin structure of the *Fab-7* boundary region

Like *Mcp*, deletions which remove the *Fab-7* boundary transform one abdominal segment, in this case A6, into a more posterior abdominal segment, in this case A7. This phenotypic transformation appears to be due to the ectopic activation of the *iab-7 cis*-regulatory domain in the parasegment in which *iab-6* normally functions, namely parasegment 11 (23). In previous studies we used genomic Southerns to analyze three overlapping deletions, $Fab\text{-}7^{1}$, $Fab\text{-}7^{2}$, and $Fab\text{-}7^{3}$, which affect *Fab-7* boundary function. The approximate breakpoints of these deletions (mapped by genomic Southern) is shown in Fig. 1C (22). To extend this analysis, we have determined the sequence of the wild type *Fab-7* region and this data is presented in Fig. 4B. We have also cloned DNA from the three *Fab-7* deficiencies, and localized by sequencing the proximal breakpoint of $Fab\text{-}7^{1}$, the distal breakpoint of $Fab\text{-}7^{3}$ and both breakpoints of the smallest deficiency, $Fab\text{-}7^{2}$. These breakpoints are indicated in the *Fab-7* sequence presented in Fig. 4B, and are shown diagrammatically in Fig. 3B. Fig. 3B also shows a map of the chromatin organization of the *Fab-7* region aligned with the DNA sequence (see 22 and data not shown).

The *Fab-7* boundary, like *Mcp*, has an unusual chromatin structure; however, the nucleoprotein organization of the *Fab-7* DNA segment appears to be considerably more complex than *Mcp*. Instead of one major hypersensitive region, *Fab-7* contains 3 major hypersensitive regions and several minor hypersensitive sites (see map in Fig. 3B). The strongest of the minor nuclease hypersensitive sites (indicated by * in Fig. 3B) is located between ~1,360 bp and ~1,500. It is separated from the first major hypersensitive region, region I, by a relatively large nuclease resistant DNA segment of ~300 bp. Hypersensitive region I spans a DNA segment of nearly 400 bp and it is located between ~1,800 bp and ~2,170 bp. It is followed by a ~160 bp nuclease resistant region which would be just large enough to contain a nucleosome core particle. Hypersensitive region II is smaller (~175 bp) than region I, and maps between ~2,325-bp and ~2,500 bp. It is followed by a nuclease resistant region of ~175 bp. Finally hypersensitive region III extends from ~2,675 bp to 2,900 bp.

The genetic properties of the *Fab-7* deletions would also suggest that the organization of functional sequences in the *Fab-7* boundary may be somewhat more complex than *Mcp*. While the three *Mcp* deletion mutants are phenotypically equivalent, this is not the case for the three *Fab-7* deletions. The most complete phenotypic transformation of PS11 into PS12 is observed in the original *Fab-7* allele, $Fab\text{-}7^{1}$. As indicated in Fig. 3B, this mutant deletes all three of the prominent nuclease hypersensitive regions, plus the most of the flanking minor hypersensitive sites. Although $Fab\text{-}7^{3}$ is a strong allele, animals carrying this mutant occasionally have clones of cells in PS11 that are not transformed. As indicated in Fig. 3B, this deletion removes the major hypersensitive regions I and II and all of the minor hypersensitive sites on the proximal side. However, in contrast to $Fab\text{-}7^{1}$, hypersensitive region III and the minor sites on the distal side are intact in $Fab\text{-}7^{3}$. Finally $Fab\text{-}7^{2}$ appears to retain partial *Fab-7* boundary function as the phenotypic transformation of PS11 into PS12 in this mutant is incomplete. The $Fab\text{-}7^{2}$ deletion is only 789 bp in length. On the distal side, the breakpoint of $Fab\text{-}7^{2}$ is within a few nucleotides of $Fab\text{-}7^{3}$. On the proximal side the breakpoint is just to the left of hypersensitive region I. Thus in this mutant, hypersensitive regions I and II are deleted, while the minor nuclease hypersensitive site (*) on the proximal side and hypersensitive region III on the distal side are retained.

DISCUSSION

Mutations which delete the *Mcp* and *Fab-7* DNA segments in the bithorax complex have a dominant gain-of-function phenotype: each transforms *one* parasegment in the abdomen into a copy of the parasegment immediately posterior. In the case of *Mcp*, PS9 is transformed into PS10 while for *Fab-7* PS11 is transformed into PS12 (23, 24). These phenotypic transformations appear to be due to the expression of the *Abd-B* gene in the affected parasegment in a pattern that is appropriate for the parasegment immediately posterior. Indeed, *Abd-B* antibody staining of *Fab-7* mutant embryos reveals that the pattern of *Abd-B* expression in PS11 is identical to that observed in PS12. On the other hand, *Abd-B* expression in PS12 is not affected in *Fab-7* mutant embryos, and the pattern is the same as that observed in PS12 of wild type embryos. *Abd-B* antibody staining of *Mcp* mutant embryos gives similar results (21, 22, 28).

Perhaps the simplest model to explain the dominant gain-of-function phenotypes of the *Mcp* and *Fab-7* mutations is that these DNA segments contain parasegment specific negative regulators or silencers—*Mcp* would be a PS9 specific silencer while *Fab-7* would be a PS11 specific silencer. In this view, *Mcp* would prevent the positive regulators in *iab-5* (which are responsible for activating *Abd-B* in PS10) from turning on the *Abd-B* gene in PS9. Similarly, the silencers associated with *Fab-7* would prevent the PS12 specific positive regulators in *iab-7* from acting on *Abd-B* in PS11. This model would predict that the dominant gain-of-function phenotypes of *Mcp* and *Fab-7* should be reverted by mutations that inactivate the positive regulators in *iab-5* and *iab-7*, respectively. Indeed, deletions or other rearrangements which disrupt *iab-5* and *iab-7* revert the *Mcp* and *Fab-7* dominant gain-of-function phenotypes. A second prediction of this model is that the dominant gain-of-function phenotype of *Mcp* and *Fab-7* should not be reverted by mutations which disrupt, respectively, *iab-4* and *iab-6*. In this case, the positive regulators in *iab-5* and

iab-7 would still be present and they would still be able to inappropriately activate *Abd-B*. However, contrary to this expectation, mutations which disrupt *iab-4* and *iab-6* can also revert *Mcp* and *Fab-7*, apparently preventing the regulatory elements in *iab-5* and *iab-7* from functioning inappropriately in PS9 and PS11 (23, 24).

The reversion of the gain-of-function phenotypes of *Mcp* and *Fab-7* by mutations that inactivate *iab-4* and *iab-6*, respectively, lead to the idea that these DNA sequences may correspond to the boundaries of *cis*-regulatory domains. In this model, the *Mcp* and *Fab-7* DNA segments would function to prevent adventitious interactions between regulatory elements (positive and negative) in adjacent *cis*-regulatory domains: *iab-4* and *iab-5* for *Mcp* and *iab-6* and *iab-7* for *Fab-7*. Consistent with this boundary model, a *lac-Z* reporter, the *bluetail* transposon, inserted into *iab-7* appears to be subject to control elements in this *cis*-regulatory domain, but is insulated from control elements in the more proximal *cis*-regulatory domains *iab-5* and *iab-6* (22) Moreover, when the *Fab-7* boundary is removed, the *bluetail* transposon then responds to regulatory elements in *iab-6* (Mihaly, J., Gausz, J., Gyurkovics, H., and Karch, F. unpublished data).

Whether the *Mcp* and *Fab-7* elements are functionally equivalent to other *Drosophila* DNA segments that act as regulatory boundaries (eg., scs: 59, 60; *su(Hw)*: 62) remains to be determined. In fact, preliminary studies of DNA fragments containing the *Mcp* and *Fab-7* elements indicate that they have some rather unusual and perhaps different properties (cf., 54). For these reasons, we have used a more classical genetic approach to further delimit the DNA sequences required for *Mcp* and *Fab-7* boundary function *in situ*. Analysis of *Mcp* deficiencies defines a small 415 bp DNA segment which is deleted in all of the mutants and appears to be essential for boundary function. As shown in Fig. 3A, this essential DNA segment closely coincides with the major chromatin specific nuclease hypersensitive region. While our results indicate that this nuclease hypersensitive region is essential for *Mcp* function, it remains to be determined whether it is also sufficient. Significantly, the sequences required for *Fab-7* boundary function also have an unusual chromatin structure. However, instead of one major hypersensitive region, the *Fab-7* DNA segment contains 3 major hypersensitive regions plus several minor sites. Our analysis of *Fab-7* mutants, in particular *Fab-7*^{2}, indicates that two of these hypersensitive regions, I and II (see Fig. 3B), are required for function. However, the sequence removed in *Fab-7*^{2} may not in themselves be sufficient since this deletion mutant retains partial activity. From the breakpoints of the other *Fab-7* deletions it would appear that sequences to left of the proximal *Fab-7*^{2} breakpoint must contribute to *Fab-7* function. Potential candidate sequences would include the minor hypersensitive site indicated by the * in Fig. 3B. From the phenotype of *Fab-7*^{3} it is also possible that sequences to the right of the distal *Fab-7*^{2} breakpoint, in particular hypersensitive region III, also contribute to *Fab-7* boundary function. The unusual chromatin structures associated with the *Mcp* and *Fab-7* boundaries are present in very early embryos when the activity state of the bithorax complex in each parasegment is initially established. Since the same nuclease cutting patterns are found in late 12–24 hr embryos, it would appear that these chromatin structures persist (at least in some tissues of the embryo) into the maintenance phase of BX-C regulation. We have not examined the chromatin structure of *Mcp* and *Fab-7* during larval, pupal or adult stages; however, the unusual chromatin structures in each DNA segment are present in tissue culture cells, and consequently, it is possible that they may persist throughout much of development.

It is interesting that the nuclease hypersensitive regions in the *Mcp* and *Fab-7* DNA segments closely correlate with sequences essential for boundary function. Other putative boundary elements including a boundary from the chicken globin locus, and the *Drosophila* scs-like elements also have one or more nuclease hypersensitive regions (58–60). Moreover, recent studies on scs localize the sequences required for enhancer blocking activity to the nuclease hypersensitive regions of this element (54). We have compared the *Mcp* and *Fab-7* DNA sequences with scs and scs′ and with each other. No regions of obvious homology were noted with either scs or scs′, nor with the consensus binding site for the *su(Hw)* protein which also has boundary function (62). We did, however, note some sequence similarities between *Mcp* and *Fab-7* and these are presented in Fig. 5. The most interesting of these, A, maps to the major nuclease hypersensitive region in *Mcp* and to hypersensitive region II in *Fab-7*. Two other sequences in the major hypersensitive region of *Mcp* also show sequence similarity to *Fab-7*. Both of these map to the third nuclease hypersensitive region of *Fab-7*. Further studies will clearly be required to determine the functional significance of these and other sequences in the *Mcp* and *Fab-7* nuclease hypersensitive sites.

ACKNOWLEDGMENTS

We would like to thank Nicole Wolff, Jackie Guiard-Maffia, Benjamin Barandun, Clarberta Michelini, Apati Andrasne, Dongo Gyorgyne, Slim Chraiti, and Stella Han for technical assistance. This work was supported in part by the Swiss National Fund (3.193-0.88), the Canton of Geneva, OTKA-920 and NIH. We would especially like to acknowledge and thank the Human Frontier Science Program Organization for a grant which helped make this collaborative research project possible.

REFERENCES

1. Ingham, P.W. (1988). The molecular genetics of embryonic pattern formation in *Drosophila*. *Nature* 335: *335*, 25–34.
2. Martinez-Arias, A. and Lawrence, P. 1985. Parasegments and compartments in the Drosophila embryo. *Nature* 313: 639–642.
3. Duncan, I. 1987. The bithorax complex. *Annu. Rev. Genet.* 21: 285–319.
4. Mahaffey, J. and Kaufman, T. 1988. The homeotic genes of the Antennapedia complex and bithorax complex of *Drosophila*. In Developmental Genetics of Higher Organisms (ed. G.M. Malacinsky), 239–260. New York: MacMillan.
5. Peifer, M., Karch, F. and Bender, W. 1987. The bithorax complex—controlling segmental identity. *Genes Dev.* 1: 891–898.
6. Sanchez-Herrero, E., Casanova, J. and Morata, G. 1988. Genetic organization of the *Drosophila* bithorax complex. *Bioessays*, 8: 124–128.
7. Akam, M.E. and Martinez-Arias. 1985. The distribution of *Ultrabithorax* transcripts in *Drosophila* embryos. *EMBO J.* 4: 1689–1700.
8. Beachy, P.A., Helfand, S.L. and Hogness, D.S. 1985. Segmental distribution of bithorax complex proteins during *Drosophila* development. *Nature* 313: 545–551.
9. Celniker, S.E. and Lewis, E.B. 1987. *Transabdominal*, a dominant mutant of the bithorax complex, produces a sexually dimorphic segmental transformation in *Drosophila*. *Genes Dev.* 1: 111–123
10. Celniker, S. E., Keelan, D. J., and Lewis, E. B. 1989. The molecular genetics of the Bithorax Complex of Drosophila: Characterization of the products of the Abdominal-B domain. *Genes Dev.* 3: 1424–1435.
11. DeLorenzi, M., Ali, N., Saari, G., Henry, C., Wilcox, M. and Bienz, M. 1988. Evidence that the *Abdominal-B* r element function is conferred by a *trans*-regulatory homeoprotein. *EMBO J.* 7: 3223–3231.
12. Karch, F., Bender, W, and Weiffenbach, B. 1990. *abdA* expression in *Drosophila* embryos. *Genes Dev* 4: 1573–1587.

13. Kuziora, M.A. and McGinnis, W. 1988. Different transcripts of the *Drosophila AbdB* gene correlate with distinct genetic sub-functions. *EMBO J.* 7: 3233–3244.
14. McGinnis, W., Levine, M.S., Hafen, E., Kuroiwa,A. and Gehring,W. 1984. A conserved DNA sequence in homeotic genes of the Drosophila Antennapedia and bithorax complexes. *Nature* 308: 428–433.
15. O'Connors, M.B., Binari, R., Perkins, L.A. and Bender, W. 1988. Alternative RNA products from the *Ultrabithorax* domain of the bithorax complex *EMBO J.* 7: 435–445.
16. Sanchez-Herrero, E., Vernos, I., Marco, R. and Morata, G. 1985. Genetic organization of the *Drosophila* bithorax complex. *Nature* 313: 108–113.
17. Scott, M.P. and Weiner, A.J. 1984. Structural relationships among genes that control development: sequence homology between the Antennapedia, Ultrabithorax, and fushi tarazu loci of Drosophila. *Proc. Natl. Acad. Sci.* 81: 4115–4119.
18. White, R.A.H. and Wilcox, M. 1985. Regulation of the distribution of *Ultrabithorax* proteins in *Drosophila*. *Nature* 318: 563–567.
19. Zavortink, M. and Sakonju, S. 1989. The morphogenetic and regulatory functions of the Drosophila *Abdominal-B* gene are encoded in overlapping RNAs transcribed from separate promoters. *Genes Dev.* 3: 1969–1981.
20. Bender, W., Akam, M., Karch, F., Beachy, P.A., Peifer, M., Spierer, P., Lewis, E.B. and Hogness, D.S. 1983. Molecular genetics of the bithorax complex in *Drosophila*. *Science* 221: 23–29.
21. Celniker, S., Sharma, S., Keelan, D. and Lewis, E. 1990. The molecular genetics of the bithorax complex of *Drosophila*: *cis*-regulation in the *Abdominal-B* domain. *EMBO J.* 9: 4277–4286.
22. Galloni, M., Gyurkovics, H., Schedl, P. and Karch, F. 1993. The bluetail transposon: evidence for independent *cis*-regulatory domains and domain boundaries in the bithorax complex. *EMBO J.* 12: 1087–1097.
23. Gyurkovics, H., Gausz, J., Kummer, J. and Karch, F. 1990. A new homeotic mutation in the *Drosophila* bithorax complex removes a boundary separating two domains of regulation. *EMBO J.* 9: 2579–2585.
24. Karch, F. Weiffenbach, B., Peifer, M., Bender, W., Duncan, I., Celniker, S., Crosby, M. and Lewis, E.B. 1985. The abdominal region of the bithorax complex. *Cell* 43: 81–96.
25. Lewis, E.B. 1978. A gene complex controlling segmentation in *Drosophila*. *Nature* 276: 565–570.
26. Lewis, P.H. 1947. *Melanogaster*-New mutants: Report of Pamela H. Lewis. *Dros. Inform. Serv.* 21: 69
27. Macias, A., Casanova, J. and Morata, G. 1990. Expression and regulation of the *abd-A* gene of *Drosophila*. *Development* 110: 1197–1207.
28. Sanchez-Herrero, E. 1991. Control of the expression of the bithorax complex *abdominal-A* and *Abdominal-B* by *cis*-regulatory regions in *Drosophila* embryos. *Development* 111: 437–449.
29. Boulet, A., Lloyd, A. and Sakonju, S. 1991. Molecular definition of the morphogenetic and regulatory functions and the *cis*-regulatory elements of the *Drosophila Abd-B* homeotic gene. *Development* 111: 393–405.
30. Casanova, J., Sanchez-Herrero, E. and Morata, G. 1986. Identification and characterization of a parasegment specific regulatory element of the *Abdominal-B* gene of *Drosophila*. *Cell* 47:627–636.
31. Sanchez-Herrero, E. and Crosby, M.A. 1988. The *Abdominal-B* gene of *Drosophila melanogaster*: overlapping transcripts exhibit two different spatial distributions. *EMBO J.* 7: 2163–2173.
32. Duncan, I. 1986. Control of bithorax complex function by the segmentation gene *fushi tarazu* of *D. melanogaster*. *Cell* 47: 297–309.
33. Harding, K. and Levine, M.J. Jr. 1988. Gap genes define the limits of *Antennapedia* and *bithorax* gene expression during early development in *Drosophila*. *EMBO J.* 7: 205–214.
34. Ingham, P. and Martinez-Arias, A. 1986. The correct activation of Antennapedia and bithorax complex genes requires the *fushi tarazu* gene. *Nature* 324: 592–597.
35. Irish, V., Martinez-Arias, A. and Akam, M. 1989. Spatial regulation of the *Antennapedia* and *Ultrabithorax* homeotic genes during *Drosophila* early development. *EMBO J.* 8: 1527–1537.
36. Irvine, K., Helfland, S. and Hogness, D. 1991. The large upstream control region of the *Drosophila* homeotic gene *Ultrabithorax*. *Development* 111: 407–424.
37. Qian, S., Capovilla, M. and Pirrotta, V. 1991. The *bx* region enhancer, a distant *cis*-control element of the *Drosophila Ubx* gene and its regulation by *hunchback* and other segmentation genes. *EMBO J.* 10: 1415–1425.
38. Reinitz, J. and Levine, M. 1990. Control of the initiation of homeotic gene expression by the gap genes *giant* and *tailless* in *Drosophila*. *Devl. Biol.* 140: 57–72.
39. Simon, J., Peiffer, M., Bender, W. and O'Connors, M. 1990. Regulatory elements of the bithorax complex that control expression along the anterior-posterior axis. *EMBO J.* 9: 3945–3956.
40. Simon, J., Chiang, A., Bender, W., Shimell, M.J. and O'Connors, M. 1993. Elements of the *Drosophila* bithorax complex that mediate repression by *Polycomb* group products. *Dev. Biol.* 158. 131–144
41. White, R. and Lehmann, R. 1986. A gap gene, *hunchback*, regulates the spatial expression of *Ultrabithorax*. *Cell* 47: 311–321.
42. Zhang, C.C., Müller, J., Hoch, M., Jäckle, H. and Bienz,M. 1992. Segmental determination in *Drosophila* conferred by *hunthback* in a control region conferring *Ultrabithorax* expression boundaries. *Genes Dev.* 113: 1171–1179.
43. Breen, T.R. and Harte, P.J. 1993. *trithorax* regulates multiple homeotic genes in the bithorax and Antennapedia complexes and exerts different tissue-specific, parasegment-specific and promoter-specific effects on each. *Development* 117: 119–134.
44. Duncan, I. 1982. *Polycomblike*: a gene that appears to be required for the normal expression of the bithorax and Antennapedia gene complexes of *Drosophila melanogaster*. *Genetics* 102: 49–70.
45. Duncan, I. and Lewis, E. 1982. Genetic control of body segment differentiation in *Drosophila*. In Developmental order: Its origin and regulation. 533–554. Alan R. Liss, Inc., New York.
46. Ingham, P. 1981. *Trithorax*: a new homeotic mutation of *Drosophila melanogaster*: the role of *trx*+ after embryogenesis. *Wilhem Roux's Arch. Dev. Biol.* 190: 365–369.
47. Jürgens, G. 1985. A group of genes controlling the spatial expression of the bithorax complex in *Drosophila*. *Nature* 316: 153–155.
48. Kennison, J.A. and Tamkun, J. 1988. Dosage-dependent modifiers of *Polycomb* and *Antennapedia* mutations in *Drosophila*. *Proc. Natl. Acad. Sci. USA* 85: 8136–8140.
49. Kennison, J.A. 1993. Transcriptional activation of *Drosophila* homeotic genes from distant regulatory elements. *TIGs* 9: 75–79.
50. Paro, R. 1990. Imprinting a determined state into the chromatin of *Drosophila*. *TiIGs* 6: 416–421
51. Shearn, A. 1989. The *ash-1*, *ash-2* and *trithorax* genes of *Drosophila melanogaster* are functionally related. *Genetics* 121: 517–525.
52. Simon, J., Chiang, A. and Bender, W. 1992. Ten different *Polycomb* group genes are required for spatial control of the *abd-A* and *Abd-B* homeotic products. Development 114: 493–505.
53. Struhl, G. and Akam, M.E. 1985. Altered distribution of *Ultrabithorax* transcripts in *extra sex combs* mutant embryos of *Drosophila*. EMBO J. 4: 3259–3264.
54. Vasquez, J., Farkas, G., Gaszner, M., Udvardy, A., Muller, M., Hagstrom, K., Gyurkovics, H., Sipos, L., Gausz, J., Galloni, M., Hogga, I., Karch, F. and Schedl, P. 1994. Genetic and molecular analysis of chromatin domains. Cold Spring Harbor Symp. Quant. Biol., in press.
55. Frieschauf, A.M., Lehrach, H., Poustka, A. and Murray, N. 1983. Lambda replacement vectors carrying polylinker sequences. J. Mol. Biol. 170: 827–842.
56. Henikoff, S. 1984. Unidirectional digestion with exonuclease III creates targeted breakpoints for DNA sequencing. Gene 28: 351–359..
57. Udvardy, A and Schedl, P. 1984. Chromatin organization of the 87A7 heat shock locus of *Drosophila melanogaster*. J. Mol. Biol 172: 385–403.
58. Chung, J.H., Whiteley, M. and Felsenfeld, G. 1993. A 5' element of the chicken beta-globin domain serves as an insulator in human erythroid cells and protects against position effect in *Drosophila*. Cell 74: 505–514.
59. Kellum, R. and Schedl, P. 1991. A position-effect assay for boundaries of higher order chromosomal domains. Cell 64: 941–950
60. Kellum, R. and Schedl, P. 1992. A group of scs elements function as domain boundaries in an enhancer-blocking assay. Mol. Cell. Biol. 12: 2424–2431.
61. Udvardy, A. Maine, E. and Schedl, P. 1985. The 87A7 chromomere. Identification of novel chromatin structures flanking the heat-shock locus that may define the boundaries of higher order domain. J. Mol. Biol. 185: 341–355.
62. Roseman, R.R., Pirrotta, V., and Geyer, P.K. 1993. The *su(Hw)* protein insulates expression of the *Drosophila melanogaster white* gene from chromosomal position-effects. EMBO J. 12: 435–442.